Demonstration of Self-Starting Nonlinear Mode Locking in Random Lasers

Fabrizio Antenucci,[1,4] Giovanni Lerario,[2] Blanca Silva Fernandéz,[2] Luisa De Marco,[2] Milena De Giorgi,[2] Dario Ballarini,[2] Daniele Sanvitto,[2,*] and Luca Leuzzi[1,3,†]

[1]*CNR-NANOTEC, Institute of Nanotechnology, Soft and Living Matter Laboratory, Piazzale Aldo Moro 5, I-00185 Rome, Italy*
[2]*CNR-NANOTEC, Institute of Nanotechnology, Via Monteroni, I-73100 Lecce, Italy*
[3]*Dipartimento di Fisica, Università Sapienza, Piazzale Aldo Moro 5, I-00185 Rome, Italy*
[4]*Saddle Point Science Ltd, 71 OAKS Avenue, Worcester Park KT4 8XE, United Kingdom*

(Received 27 July 2020; accepted 24 March 2021; published 27 April 2021)

In ultrafast multimode lasers, mode locking is implemented by means of saturable absorbers or modulators, allowing for very short pulses. This occurs because of nonlinear interactions of modes with well equispaced frequencies. Though theory predicts that, in the absence of any device, mode locking would occur in random lasers, this has never been demonstrated so far. Through the analysis of multimode correlations we provide clear evidence for nonlinear mode coupling in random lasers. The behavior of multiresonance intensity correlations is tested against the nonlinear frequency matching condition equivalent to the one underlying phase locking in ordered ultrafast lasers. Nontrivially large correlations are clearly observed for spatially overlapping resonances that sensitively depend on the frequency matching condition to be satisfied, eventually demonstrating the occurrence of nonlinear mode-locked mode coupling. This is the first example, to our knowledge, of an experimental realization of self-starting mode locking in random lasers, allowing for many new developments in the design and use of nanostructured devices.

DOI: 10.1103/PhysRevLett.126.173901

When light propagates through a random medium, the electromagnetic field provides a complicated emission pattern as light undergoes multiple scattering. In random lasers [1–8] such scattering allows for population inversion under external pumping. Random lasers are made of an optically active medium, providing gain, and randomly placed scatterers, providing the high refraction index and the feedback mechanism leading to amplification by stimulated emission. They do not require complicated construction and rigid optical alignment, have a low cost, undirectional emissions, high operational flexibility and give rise to a number of promising applications in the field of speckle-free imaging [9,10], remote sensing [11,12], medical diagnostics [13–16] and optoelectronic devices [17,18]. Many works have been devoted to the random laser mode control, e.g., by tuning concentration of scatterers [2], by changing pumping profile [19] or temperature [20,21], and else gain material [22] in a number of diverse approaches [23–25]. Effective engineered control requires a deep knowledge of the physical mechanisms underlying the behavior of random lasers. Here we investigate one of these mechanisms in the presence of intrinsic, nonperturbative, randomness.

We exploit a statistical mechanical model of light modes interacting in a random medium excited by external pumping to extract information about fundamental mechanisms of a random laser. Our aim is understanding whether a random laser built without specific technological requirements exhibits the basic feature of standard pulsed lasers: *mode locking*. Standard laser theory shows that the dominant mode interaction above threshold is highly nonlinear [26]. In the random laser case, mode couplings are predicted to be disordered, both in the interaction network and in the coupling values. Therefore, the understanding of cross-mode interactions is an open issue and fundamental questions need to be answered about their strength, sign, and number of simultaneously involved modes.

Clearly, modes must spatially overlap to display mode locking [27–29], as observed in experiments on specifically designed random lasers, where pairwise (linear) interaction manifests because of two modes competition for the overall intensity within the same optical volume [19]. In Ref. [30] a step towards nonlinear mode locking was taken, including a graphene saturable absorber to yield a quasi mode locking of coherent feedback in random fiber laser. With the assistance of the saturable absorber, resonant modes are selected and mode locked. Spatial overlap is not, however, a sufficient condition for interaction, nor does it provide any information about the coupling values. At the same time, the exact structure of the spatial distribution of the modes in most random lasers is hard to determine, which makes a quantitative analysis of the interacting parameters rather hard. Eventually, there is no saturable absorber in random lasers and a possible nonlinear matching of frequencies, that is, the locking of more than two modes, would occur as a self-starting phenomenon [31].

We have developed an analysis of random systems of interacting light modes providing information about the

mode-coupling constants and applied it to the emission spectra of a GaAs powder-based random laser, experimentally demonstrating the nonlinear coupling of spatially overlapping modes and its mode-locking nature.

Although the mode-locking phenomenon is known to be nonlinear and light modes are expected to be coupled, the mechanism and nature of this nonlinear coupling in random lasers has never been experimentally tested. The theory for stationary regimes in a random laser consists in an effective stochastic nonlinear potential dynamics for the mode slow amplitudes $a(t)$ (see Supplemental Material [32]) whose Hamiltonian reads

$$\mathcal{H} = -\sum_{\mathbf{k}_2|\mathrm{FMC}(\mathbf{k})} g^{(2)}_{k_1k_2} a_{k_1} a^*_{k_2} - \frac{1}{2}\sum_{\mathbf{k}_4|\mathrm{FMC}(\mathbf{k})} g^{(4)}_{k_1k_2k_3k_4} a_{k_1} a^*_{k_2} a_{k_3} a^*_{k_4} + \mathrm{c.c.}, \quad (1)$$

where FMC stands for the frequency matching condition,

$$|\omega_{k_1} - \omega_{k_2} + \omega_{k_3} - \omega_{k_4}| < \gamma; \qquad \gamma \equiv \sum_{j=1}^{4} \gamma_{k_j}, \quad (2)$$

where ω_k is the angular frequency of the mode k and γ_k's are the linewidths of the resonances. Further complexity of the mode interaction is comprised inside the coupling coefficients

$$g^{(4)}_{k_1k_2k_3k_4} \propto \int_V d\boldsymbol{r}\hat{\chi}^{(3)}(\boldsymbol{r};\omega_{k_1},\omega_{k_2},\omega_{k_3},\omega_{k_4}) \vdots \boldsymbol{E}_{k_1}(\boldsymbol{r})\boldsymbol{E}_{k_2}(\boldsymbol{r})\boldsymbol{E}_{k_3}(\boldsymbol{r})\boldsymbol{E}_{k_4}(\boldsymbol{r}), \quad (3)$$

where $\hat{\chi}^{(3)}$ is the nonlinear susceptibility tensor of the medium and $\boldsymbol{E}_k(\boldsymbol{r})$ is the eigenmode of frequency ω_k.

In standard lasers FMC is induced by nonlinear devices [26] and it induces phase locking [33–35] and ultrashort pulses [26,36–41]. In random lasers no *ad hoc* device is present in the resonator and even the definition of *resonator* is far from straightforward [42]. Consequently, mode locking would be, in this case, *a self-starting phenomenon* due to randomness.

Contrarily to standard multimode lasers [43,44], in random lasers mode locking cannot be identified by an overall temporal optical pulse (though each mode has a time dynamics following the pumping pulse [45]). This comes about because the frequencies of the lasing modes are not equispaced and, therefore, their convolution does not give rise to a pulse $I(t)$ in time. This can be explicitly seen in theoretical models where mode locking is implemented together with unperturbative randomness [46,47]. We therefore demonstrate a different approach to detect it, based on intensity cross-correlation measurements of a GaAs random laser modes at different wavelengths.

Our random laser is composed by a thin deposition of GaAs powder, whose properties are reported in the Supplemental Material [32], which includes Ref. [48]. A Gaussian laser beam (780 nm excitation wavelength) illuminates the sample propagating perpendicular to the deposition plane (x, y). The detection line is along the z direction in transmission configuration (i.e., at the opposite side of the sample with respect to the excitation line). The sample thickness is irregular in the z direction, though always thinner than 100 μm (details in the Supplemental Material [32]).

The emission intensity in random lasers is typically too low to allow a good resolution in all dimensions (x, y, λ) within a single shot. In our experiments we have emission spectra from a given slice of the sample (10 μm wide) resolved in the x coordinate (x, λ) for 100, 1000, and 10000 shots, corresponding to 10, 100, 1000 ms integration time. These acquisition times allowed us to obtain a spectral resolution high enough to adequately probe the presence of nonlinear interaction. An instance of a space-wavelength spectrum is displayed in the top panel of Fig. 1.

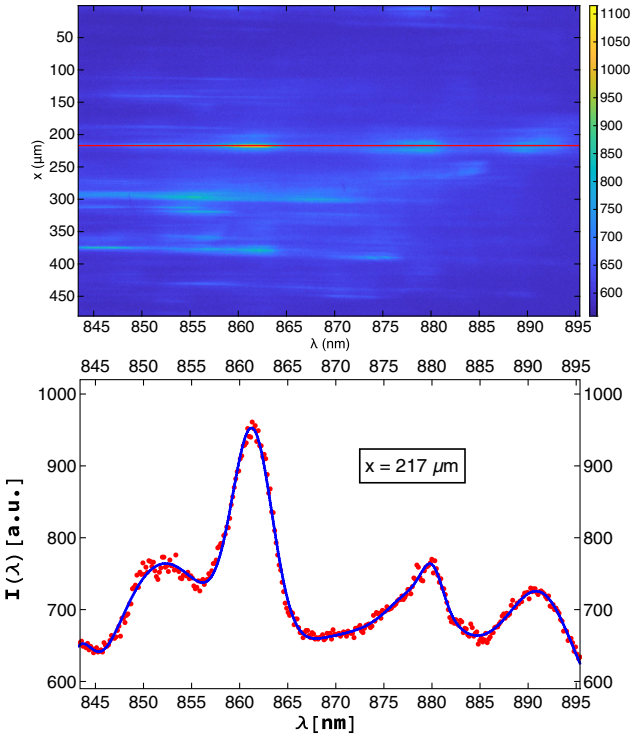

FIG. 1. (Top panel) Instance of an intensity spectrum vs position and wavelength of a GaAs crystal powder sample with 10 ms data acquisition time (100 shots). The red line represents the section of the spectrum at position $x = 217$ μm that is displayed in the bottom panel. (Bottom panel) The red points are the intensity spectrum vs wavelength λ at coordinate $x = 217$ μm, corresponding to the red cut in the top 2D plot. The blue continuous curve is a multi-Gaussian interpolation with a weighted combination of $N_G = 7$ Gaussian curves. In this instance $N_G = 7$ turns out to be the number yielding the largest likelihood with data avoiding overfitting (see Supplemental Material [32]).

In order to detect nonlinear mode coupling by a statistical analysis we first have to identify and characterize mode resonances. In all acquired spectra at all available positions (x) resonances are identified by multiple fitting with linear combinations of a variable number of Gaussian distributions chosen according to the Akaike Information Criterion (see Supplemental Material [32]). An instance of this procedure is reported in Fig. 1, bottom panel, where we plot raw data (in red dots) and compare them to a multi-Gaussian interpolating function. Eventually, we build a complete list of all resonances for each spectrum produced in each one of the different data acquisitions $t = 1, \ldots, N_{\text{spectra}} = 1000$ in the series of measurements. Each intensity peak $I_k^{(t)}$ of the spectrum t is identified by its angular frequency ω_k, its linewidth γ_k, its position x_k, and the FWHM Δx_k in its position coordinate: $I_k^{(t)} \equiv I^{(t)}(x_k, \Delta x_k; \omega_k, \gamma_k)$.

Once we have the resonances we must study their correlations. Since our aim is to detect nonlinear interactions we have to go beyond the standard analysis of intensity correlations in random media [49,50] and consider the multipoint intensity correlations related to the $\chi^{(3)}$ nonlinearity, i.e., the four-points correlations. We then collect all quadruplets of intensity resonances I_j, I_k, I_l, I_m occurring in the N_{spectra} spectra. A single quadruplet (i, j, k, l) occurs in more spectra, if not in all, though in each spectrum the intensities fluctuate, eventually providing a statistical ensemble of quadruplets. For each quadruplet we compute the intensity four point connected correlation function

$$c_4(\omega_j, \omega_k, \omega_l, \omega_m) = \frac{\langle I_j I_k I_l I_m \rangle_c}{\sigma_j \sigma_k \sigma_l \sigma_m} \tag{4}$$

with $\sigma_j = \langle I_j^2 \rangle - \langle I_j \rangle^2$ and where the average $\langle (\ldots) \rangle$ is taken over the ensemble of the realizations of the given quadruplet (i, j, k, l) in the many emissions acquired.

The function c_4 is a cumulant: it has the property of being small when the resonances are (nonlinearly) uncorrelated and large when they are very correlated (see Supplemental Material [32]). Indeed, it is zero whenever the intensity variables can be divided into two independent sets, so that it is apt to detect the nonlinear properties of the random laser (where the two-point intensity-intensity correlations [50] would not suffice). We can, then, discriminate between small and large looking at the distribution of values of these intensity correlations. However, because of the many spurious effects contributing to correlation among modes, in order to identify anomalously large correlations due to mode coupling we first need a reference for what *small* means, which we will term background (BG) correlation. Therefore, we analyze the distributions of the c_4 in a sample dataset composed by all sets of four distinct modes, each one of them pertaining to a *different* spectrum. In this case no contribution to intensity correlation can be induced by interaction of modes competing for the energy pumped into the system.

We, consequently, compute the distribution of the c_4 values of all sets of four different resonances occurring at the same position x in the same spectrum, that we call the self-overlapping intensity resonances (SOIR), and of all sets of four intensity peaks of modes at different wavelength *and* at different x in the same spectrum, i.e., the nonoverlapping intensity resonances (NOIR).

In Fig. 2 we display the distributions of the SOIR correlation functions c_4 (top), of the NOIR c_4 (mid) and of the BG c_4 (bottom). According to Eq. (3), sets of SOIR might be induced by nonlinearly interacting modes because their space overlap is certainly nonzero. Sets of NOIR might still be related to interacting modes in an extended mode scenario where $\boldsymbol{E}_k(\boldsymbol{r}) \neq 0$ for $\boldsymbol{r}$ in a large portion of space [51].

The largest values appear always on the SOIR sets. Comparing the distributions in Fig. 2 as the number of acquired emissions increases, the dominion of possible values for the SOIR correlations extends its extremes in the tails of the distribution, while the distributions of NOIR and background c_4 appear insensitive to the change in acquisition time. Moreover, no difference can be appreciated between distributions of c_4 of NOIR and BG resonances (cf. Fig. 2). Thus, even if extended modes could be present in the sample, the present analysis cannot discriminate weak long-range mode coupling with respect to noise.

In Fig. 3 we superimpose instances of the normalized distributions for the background, the NOIR and the SOIR correlations for an acquisition time of 100 ms, clearly showing that the tails of the SOIR distribution extend well beyond the 3σ of the other two. With extremely high confidence, we can, finally, operatively identify nonlinearly *interacting* sets of modes as those whose multimode correlation is larger than the 3σ of the background correlation distribution and we can conclude that spatially overlapping modes interact nonlinearly in the random lasing regime.

Do the interacting modes (SOIR with large c_4) also satisfy FMC (2)? To test it we introduce a "FMC parameter"

$$\Delta_4 \equiv \frac{|\omega_1 - \omega_2 + \omega_3 - \omega_4|}{\gamma_1 + \gamma_2 + \gamma_3 + \gamma_4} \tag{5}$$

representing the frequency matching (*un*)satisfaction. The smaller Δ_4, the better the matching among angular frequencies of four modes. To relate interaction and mode locking we, then, look for a direct link between small Δ_4 values and very large intensity correlations, in the tails of the SOIR distribution $P(c_4)$.

In order to understand the relationship between mode locking and couplings we analyze the behavior of the mean

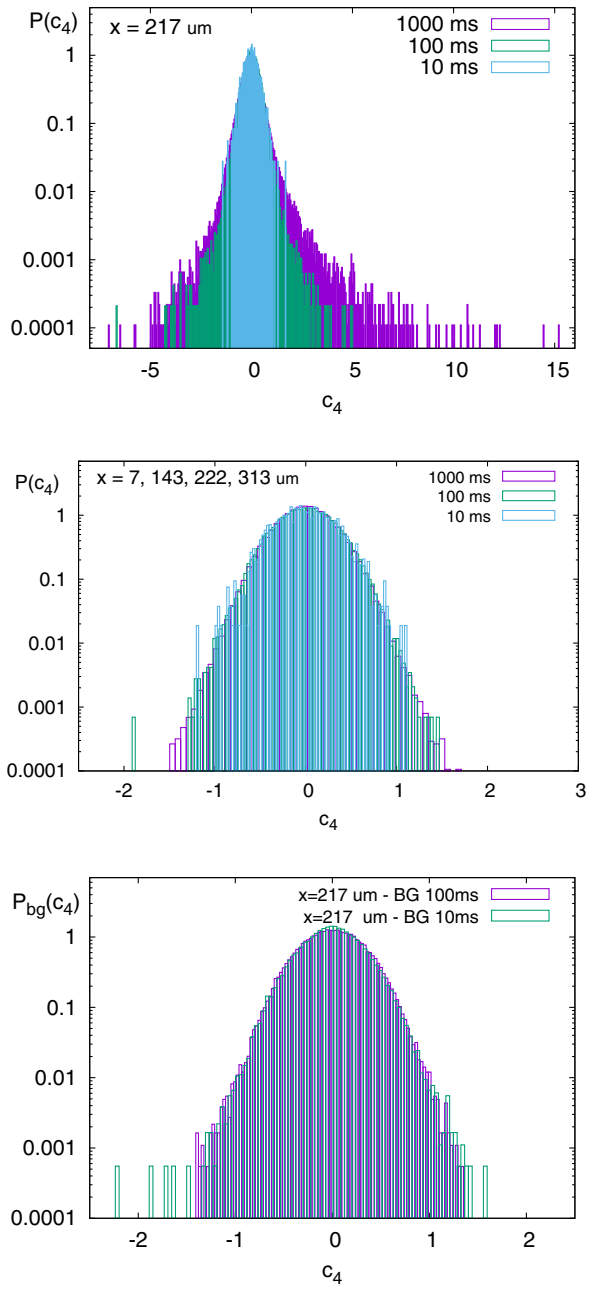

FIG. 2. Normalized distribution of c_4 for acquisition times 10, 100, 1000 ms: (top) c_4 taken at the same acquired spectrum, same position x, SOIR; (mid) c_4 taken at the same spectrum, but different positions x, NOIR; (bottom) c_4 taken at different acquired spectra, same x, BG.

square displacement σ_{c_4} of the distribution computed exclusively on those quadruplets whose frequencies yield Δ_4 values in a given interval (of width 0.01). In Fig. 4 we plot the σ_{c_4} of the distributions of correlations among SOIR, NOIR, and BG sets versus Δ_4. We observe *no* dependence on Δ_4 for BG and NOIR correlations. On the contrary, the σ_{c_4} of SOIR correlations decreases with Δ_4. In the top panel of Fig. 2 and in Fig. 3 we saw that the SOIR distributions have large tails, corresponding to interacting

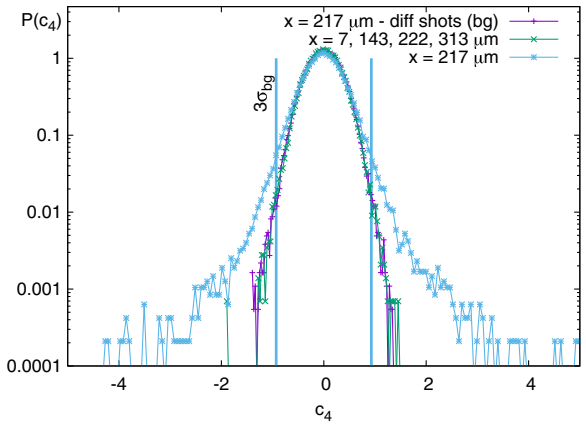

FIG. 3. Normalized distributions of c_4 at acquisition time 100 ms for background correlations, nonoverlapping resonance correlations and spatial overlapping resonance correlations. The vertical lines correspond to $\pm 3\sigma$ of the background correlation distribution.

sets. In view of such $\sigma_{c_4}(\Delta_4)$ behavior we now understand that large correlations (in distributions with large σ) are due to contributions from the histogram sections at small Δ_4. In Figs. 4, 5 we see that increasing Δ_4 the σ_{c_4} of the SOIR correlation becomes of the order of the one of the background and this means that nontrivially strong correlations only occur when frequencies are locked.

This behavior occurs at all acquisition times used in experiments, cf. Fig. 5. In Fig. 5 we call Δ_4^{ML} the value below which surely interacting modes can be neatly discriminated from background correlation. We observe that Δ_4^{ML} decreases, decreasing the acquisition time. According to Eq. (2), in the limit of the single shot experiment, interaction would be allowed only among

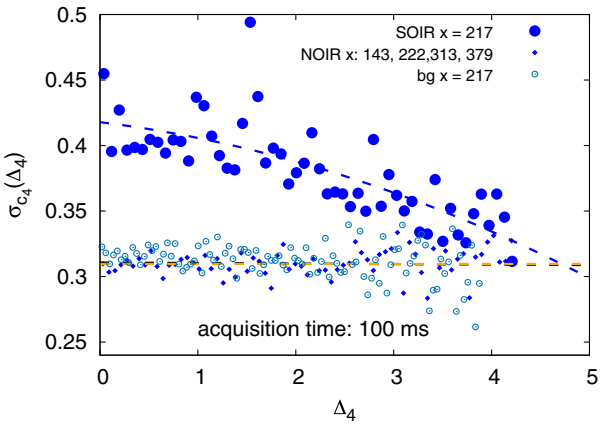

FIG. 4. Mean square displacements σ_{c_4} of the $P(c_4)$ at fixed Δ_4 intervals for various distributions. The binning of Δ_4 is 0.01. σ_{c_4} of the distributions of correlations on quadruplets of SOIR (large full points), NOIR (small full points), and BG resonances (small empty points) is displayed vs Δ_4 at 100 ms acquisition time. The SOIR and BG resonances in the plot are taken at pixel $x = 217$ μm.

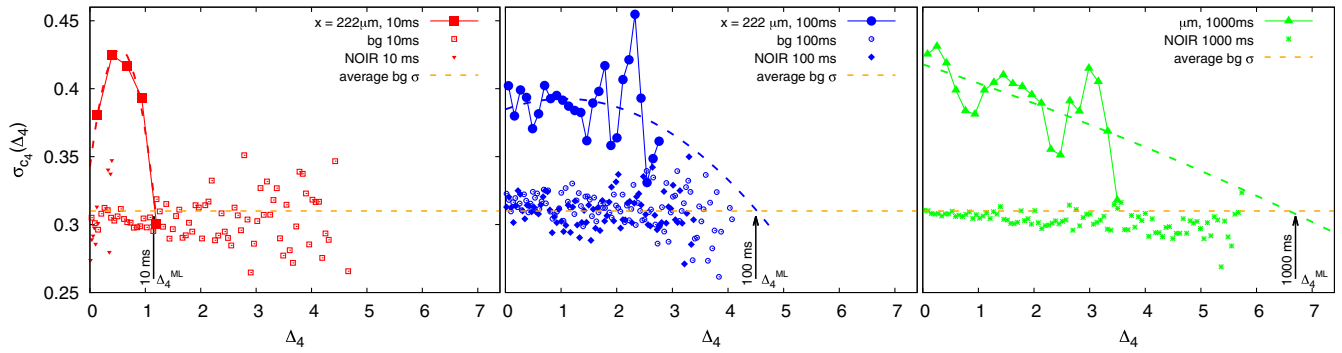

FIG. 5. Mean square displacement σ_{c_4} of the $P(c_4)$ at fixed FMC parameter Δ_4 intervals for distributions at acquisition times 10 (left, red), 100 (mid, blue), and 1000 ms (right, green). SOIR quadruplets are taken from spectra at position $x = 222$ μm. Background and NOIR correlations do not show any dependence on FMC, whereas SOIR correlation distributions tend to shrink as the FMC is progressively relaxed. Dashed lines are parabolic interpolations of SOIR $\sigma_{c_4}(\Delta_4)$ behaviors. The boundary value Δ_4^{ML} at which SOIR σ's decreases to values of the order of background σ's depends on the acquisition time. In particular, Δ_4^{ML} decreases with the number of shots, towards the expected limit of $\Delta_4^{\mathrm{ML}} \lesssim 1$ for a single shot.

those modes whose energies satisfy the FMC relationship. In terms of data reported in Fig. 5 this would imply that a relevant fraction of interacting mode sets should appear for $\Delta_4 \lesssim O(1)$. The outcome reported is strongly compatible with such a requirement and is a strong evidence for mode locking in random lasers.

Eventually, we also checked (see Supplemental Material [32]) that the frequency matching influence is not an artifact of the statistical sample size: the quantity of identified resonances does not play a role in the frequency matching dependence (parameter Δ_4) of the c_4 distribution.

Summing up, in our study on multi-intensity correlations we first identified as certainly interacting quadruplets those composed by modes whose intensity correlation lies in the long tails of the distribution $P_{\mathrm{SOIR}}(c_4)$, cf. top panel of Fig. 2. We notice that large tails in (and exclusively in) the $P_{\mathrm{SOIR}}(c_4)$ occur varying the pumping power, as well (see Supplemental Material [32]). Then, we observed (Figs. 4 and 5) that the FMC (2) appears to play a determinant role in the distribution of the correlation of intensities of interacting sets of modes (thick points in Figs. 4, 5), and only on those, leading to the conclusion that mode locking actually take places in random lasers.

This is the same mechanism behind the nonlinear mode coupling in ordered multimode lasers, though without any *ad hoc* device like a saturable absorber or a modulator: a self-starting mechanism induced by randomness.

To unveil the self-starting mechanism beyond the just demonstrated locking of modes in random lasers mandatorily requires the identification of *mode phases*. We believe that the presented results might be a significant step to stimulate and lead the theoretical understanding and the experimental procedures necessary to provide a protocol to determine mode phases in random lasers.

As a last remark we recall that in the ordered case mode locking induces ultrafast pulses. In random lasers, instead, no train of pulses is present, because the distribution of frequencies is random, rather than comblike [33], and in the subclass of *glassy* random lasers [52,53] even equispaced frequencies would not be enough to provide pulses [47].

The presence of self-starting mode locking opens the way to novel applications of random lasers. One example is the possibility of pulsed random lasers. In this case the disorder should be tuned to have a spectrum whose resonances are reasonably equispaced.

Indeed, in standard pulsed laser [26] it is the combination of comblike spectra [39] and nonlinear frequency matching [54] that yields intensity pulses in the time domain [33,55]. This is a far nontrivial challenge but impressive development in nanostructure and photonic crystal design (see, e.g., Refs. [23–25]) might make such a construction feasible in the near future.

Another example is in the field of reservoir computing [56–58]. In this paradigm one exploits the intrinsic dynamics of a "reservoir" to perform the desired computations. The reservoir is only required to display sufficiently complex dynamics that are then mapped by a readout layer onto a low-dimensional space. In addition to the nonlinear response of the emission in the random lasing regime, the existence of nonlinear interactions among modes makes random lasers a promising platform for reservoir computing in order to outperform linear classifiers [59].

The authors thank D. Ancora, G. Gradenigo, M. Leonetti, and A. Marruzzo for useful discussions, D. Cannoletta for XRD measurements and A. Fieramosca for SEM images. The research leading to these results has received funding from the Italian Ministry of Education, University and Research under the PRIN2015 program, Grant No. 2015K7KK8L-005, and the PRIN2017 program, Grant No. 2017P9FJBS, from the European Research Council (ERC) under the European Union's Horizon 2020 research and innovation program, project

ElecOpteR Grant Agreement No. 780757 and project LoTGlasSy, Grant Agreement No. 694925, from Fondo Integrativo Speciale per la Ricerca—C. N. R. Tecnopolo di nanotecnologia e fotonica per la medicina di precisione and from Regione Puglia, "Progetto Tecnopolo per la Medicina di precisione," DGR n. 2117.

*daniele.sanvitto@cnr.it
†luca.leuzzi@cnr.it

[1] H. Cao, Y. G. Zhao, S. T. Ho, E. W. Seelig, Q. H. Wang, and R. P. H. Chang, Random Laser Action in Semiconductor Powder, Phys. Rev. Lett. **82**, 2278 (1999).
[2] H. Cao, J. Y. Xu, S. H. Chang, and S. T. Ho, Transition from amplified spontaneous emission to laser action in strongly scattering media, Phys. Rev. E **61**, 1985 (2000).
[3] D. S. Wiersma, The physics and applications of random lasers, Nat. Phys. **4**, 359 (2008).
[4] J. Andreasen, A. A. Asatryan, L. C. Botten, B. A. Byrne, H. Cao, L. Ge, L Labonté, P. Sebbah, A. D. Stone, H. E. Türeci, and C. Vanneste, Modes of random lasers, Adv. Opt. Photonics **3**, 88 (2011).
[5] H. Cao, Y. G. Zhao, H. C. Ong, S. T. Ho, J. Y. Dai, J. Y. Wu, and R. P. H. Chang, Ultraviolet lasing in resonators formed by scattering in semiconductor polycrystalline films, Appl. Phys. Lett. **73**, 3656 (1998).
[6] M. Anni, S. Lattante, T. Stomeo, R. Cingolani, G. Gigli, G. Barbarella, and L. Favaretto, Modes interaction and light transport in bidimensional organic random lasers in the weak scattering limit, Phys. Rev. B **70**, 195216 (2004).
[7] K. L. van der Molen, R. W. Tjerkstra, A. P. Mosk, and A. Lagendijk, Spatial Extent of Random Laser Modes, Phys. Rev. Lett. **98**, 143901 (2007).
[8] A. Tulek, R. C. Polson, and Z. V. Vardeny, Naturally occurring resonators in random lasing of π-conjugated polymer films, Nat. Phys. **6**, 303 (2010).
[9] B. Redding, A. A. Choma, and H. Cao, Speckle-free laser imaging using random laser illumination, Nat. Photonics **6**, 355 (2012).
[10] M. Barredo-Zuriarrain, I. Iparraguirre, J. Fernández, J. Azkargorta, and R. Balda, Speckle-free near-infrared imaging using a nd3+ random laser, Laser Phys. Lett. **14**, 106201 (2017).
[11] E. Ignesti, F. Tommasi, L. Fini, F. Martelli, N. Azzali, and S. Cavalieri, A new class of optical sensors: A random laser based device, Sci. Rep. **6**, 35225 (2016).
[12] Y. Xu, L. Zhang, S. Gao, P. Lu, S. Mihailov, and X. Bao, Highly sensitive fiber random-grating-based random laser sensor for ultrasound detection, Opt. Lett. **42**, 1353 (2017).
[13] R. C. Polson and Z. V. Vardeny, Random lasing in human tissues, Appl. Phys. Lett. **85**, 1289 (2004).
[14] Q. Song, S. Xiao, Z. Xu, J. Liu, X. Sun, V. Drachev, V. M. Shalaev, O. Akkus, and Y. L. Kim, Random lasing in bone tissue, Opt. Lett. **35**, 1425 (2010).
[15] F. Lahoz, I. R. Martín, M. Urgellés, J. Marrero-Alonso, R. Marín, C. J. Saavedra, A. Boto, and M. Díaz, Random laser in biological tissues impregnated with a fluorescent anticancer drug, Laser Phys. Lett. **12**, 045805 (2015).
[16] Y. Wang, Z. Duan, Z. Qiu, P. Zhang, J. Wu, D. Zhang, and T. Xiang, Random lasing in human tissues embedded with organic dyes for cancer diagnosis, Sci. Rep. **7**, 8385 (2017).
[17] D. T. W. Lin, Y. C. Hu, and C. Cheng, The optimization of the thermal response on the zno flexible pyroelectric film temperature sensor, IEEE Sens. J. **12**, 397 (2012).
[18] Y.-M. Liao, Y.-C. Lai, P. Perumal, W.-C. Liao, C.-Y. Chang, C.-S. Liao, S.-Y. Lin, and Y.-F. Chen, Highly stretchable label-like random laser on universal substrates, Adv. Mat. Technol. **1**, 1600068 (2016).
[19] M. Leonetti, C. Conti, and C. Lopez, The mode-locking transition of random lasers, Nat. Photonics **5**, 615 (2011).
[20] S. Mujumdar, M. Ricci, R. Torre, and D. S. Wiersma, Amplified Extended Modes in Random Lasers, Phys. Rev. Lett. **93**, 053903 (2004).
[21] T. Zhai, Y. Zhou, S. Chen, Z. Wang, J. Shi, D. Liu, and X. Zhang, Pulse-duration-dependent and temperature-tunable random lasing in a weakly scattering structure formed by speckles, Phys. Rev. A **82**, 023824 (2010).
[22] Z. Wang, X. Shi, S. Wei, Y. Sun, Y. Wang, J. Zhou, J. Shi, and D. Liu, Two-threshold silver nanowire-based random laser with different dye concentrations, Laser Phys. Lett. **11**, 095002 (2014).
[23] Y.-J. Lee, T.-W. Yeh, Z.-P. Yang, Y.-C. Yao, C.-Y. Chang, M.-T. Tsai, and J.-K. Sheu, A curvature-tunable random laser, Nanoscale **11**, 3534 (2019).
[24] X. Shi, Q. Chang, Y. Bian, H. Cui, and Z. Wang, Line width-tunable random laser based on manipulating plasmonic scattering, ACS Photonics **6**, 2245 (2019).
[25] M. Lee, S. Callard, C. Seassal, and H. Jeon, Taming of random lasers, Nat. Photonics **13**, 445 (2019).
[26] H. A. Haus, Mode-locking of lasers, IEEE J. Quantum Electron. **6**, 1173 (2000).
[27] F. Antenucci, C. Conti, A. Crisanti, and L. Leuzzi, General Phase Diagram of Multimodal Ordered and Disordered Lasers in Closed and Open Cavities, Phys. Rev. Lett. **114**, 043901 (2015).
[28] F. Antenucci, A. Crisanti, and L. Leuzzi, Complex spherical $2+4$ spin glass: A model for nonlinear optics in random media, Phys. Rev. A **91**, 053816 (2015).
[29] F. Antenucci, *Statistical Physics of Wave Interactions* (Springer, New York, 2016).
[30] R. Ma, W. L. Zhang, X. P. Zeng, Z. J. Yang, Y. J. Rao, B. C. Yao, C. B. Yu, Y. Wu, and S. F. Yu, Quasi mode-locking of coherent feedback random fiber laser, Sci. Rep. **6**, 39703 (2016).
[31] L. Leuzzi, C. Conti, V. Folli, L. Angelani, and G. Ruocco, Phase Diagram and Complexity of Mode-Locked Lasers: From Order to Disorder, Phys. Rev. Lett. **102**, 083901 (2009).
[32] See Supplemental Material at http://link.aps.org/supplemental/10.1103/PhysRevLett.126.173901 for further information about the model theory, the material properties, the experimental details and for a deepening of the methods of data analysis.
[33] A. Marruzzo and L. Leuzzi, Nonlinear xy and p-clock models on sparse random graphs: Mode-locking transition of localized waves, Phys. Rev. B **91**, 054201 (2015).
[34] F. Antenucci, M. Ibáñez Berganza, and L. Leuzzi, Statistical physical theory of mode-locking laser generation with a frequency comb, Phys. Rev. A **91**, 043811 (2015).

[35] F. Antenucci, M. Ibañez Berganza, and L. Leuzzi, Statistical physics of nonlinear wave interaction, Phys. Rev. B **92**, 014204 (2015).

[36] A. Gordon and B. Fischer, Phase Transition Theory of Many-Mode Ordering and Pulse Formation in Lasers, Phys. Rev. Lett. **89**, 103901 (2002).

[37] O. Gat, A. Gordon, and B. Fischer, Solution of a statistical mechanics model for pulse formation in lasers, Phys. Rev. E **70**, 046108 (2004).

[38] M. Katz, A. Gordon, O. Gat, and B. Fischer, Statistical Theory of Passive Mode Locking with General Dispersion and Kerr Effect, Phys. Rev. Lett. **97**, 113902 (2006).

[39] Th. Udem, R. Holzwarth, and T. W. Hansch, Optical frequency metrology, Nature (London) **416**, 233 (2002).

[40] A. Baltuška, Th. Udem, M. Uiberacker, M. Hentschel, E. Goulielmakis, Ch. Gohle, R. Holzwarth, V. S. Yakovlev, A. Scrinzi, T. W. Hänsch, and F. Krausz, Attosecond control of electronic processes by intense light fields, Nature (London) **421**, 611 (2003).

[41] A. Schliesser, C. Gohle, Th. Udem, and T. W. Hänsch, Complete characterization of a broadband high-finesse cavity using an optical frequency comb, Opt. Express **14**, 5975 (2006).

[42] V. S. Lethokov, Generation of light by a scattering medium with negative resonance absorption, Sov. Phys. JETP **26**, 835 (1968), http://www.jetp.ac.ru/cgi-bin/dn/e_026_04_0835.pdf.

[43] R. Trebino, K. W. DeLong, D. N. Fittinghoff, J. N. Sweetser, M. A. Krumbügel, and D. J. Kane, Measuring ultrashort laser pulses in the time-frequency domain using frequency-resolved optical gating, Rev. Sci. Instrum. **68**, 3277 (1997).

[44] R. Trebino, *Frequency-Resolved Optical Gating: The Measurement of Ultrashort Laser Pulses* (Springer, New York, 2002).

[45] C. M. Soukoulis, X. Jiang, J. Y. Xu, and H. Cao, Dynamic response and relaxation oscillations in random lasers, Phys. Rev. B **65**, 041103(R) (2002).

[46] A. Marruzzo and L. Leuzzi, Multi-body quenched disordered *xy* and *p*-clock models on random graphs, Phys. Rev. B **93**, 094206 (2016).

[47] G. Gradenigo, F. Antenucci, and L. Leuzzi, Glassiness and lack of equipartition in random lasers: The common roots of ergodicity breaking in disordered and nonlinear systems, Phys. Rev. Research **2**, 023399 (2020).

[48] M. Dryga, P. Jele, M. Radecka, and J. F. Janik, Ammonolysis of polycrystalline and amorphized gallium arsenide gaas to polytype-specific nanopowders of gallium nitride gan, RSC Adv. **6**, 41074 (2016).

[49] S. Feng, C. Kane, P. A. Lee, and A. Douglas Stone, Correlations and Fluctuations of Coherent Wave Transmission Through Disordered Media, Phys. Rev. Lett. **61**, 834 (1988).

[50] J. F. de Boer, M. P. van Albada, and A. Lagendijk, Transmission and intensity correlations in wave propagation through random media, Phys. Rev. B **45**, 658 (1992).

[51] J. Fallert, R. J. B. Dietz, J. Sartor, D. Schneider, C. Klingshirn, and H. Kalt, Co-existence of strongly and weakly localized random laser modes, Nat. Photonics **3**, 279 (2009).

[52] N. Ghofraniha, I. Viola, F. Di Maria, G. Barbarella, G. Gigli, L. Leuzzi, and C. Conti, Experimental evidence of replica symmetry breaking in random lasers, Nat. Commun. **6**, 6058 (2015).

[53] I. Viola, L. Leuzzi, C. Conti, and N. Ghofraniha, Basic Physics and Recent Developments of Organic Random Lasers, in *Organic Lasers*, edited by M. Anni and S. Lattante (Jenny Stanford Publishing, Boca Raton, 2018).

[54] M. Sargent III, M. O'Scully, and W. E. Lamb, *Laser Physics* (Addison Wesley Publishing Company, Reading, MA, 1978).

[55] T. Brabec and F. Krausz, Intense few-cycle laser fields: Frontiers of nonlinear optics, Rev. Mod. Phys. **72**, 545 (2000).

[56] D. Verstraeten, B. Schrauwen, M. D' Haene, and D. Stroobandt, An experimental unification of reservoir computing methods, Neural Netw. **20**, 391 (2007).

[57] G. van der Sande, D. Brunner, and M. C. Saoriano, Advances in photonic reservoir computing, Nanophotonics **6**, 561 (2017).

[58] K. Nakajima, Physical reservoir computing? An introductory perspective, Jpn. J. Appl. Phys. **59**, 060501 (2020).

[59] D. Ballarini, A. Gianfrate, R. Panico, A. Opala, S. Ghosh, L. Dominici, V. Ardizzone, Milena D. Giorgi, G. Lerario, G. Gigli, Timothy C. H. Liew, M. Matuszewski, and D. Sanvitto, Polaritonic neuromorphic computing outperforms linear classifiers, Nano Lett. **20**, 3506 (2020).